Journal of Science and Transport Technology
Journal homepage: https://jstt.vn/index.php/en

Used Coffee Grounds as Fine Aggregate in Lightweight Geopolymer Composites: Influence on Engineering Properties and Microstructures

Viet-Hung Vu[1], Quoc-Dung Huynh[2], Thao-Van Vo[3], Trong-Phuoc Huynh[2,*]
[1]Faculty of Civil Engineering, Campus in Ho Chi Minh City, University of Transport and Communications, 450-451 Le Van Viet Street, Tang Nhon Phu Ward, Ho Chi Minh City, Vietnam
[2]Faculty of Civil Engineering, College of Engineering, Can Tho University, Campus II, 3/2 Street, Ninh Kieu Ward, Can Tho City 94000, Vietnam
[3]Faculty of Civil Engineering, Ton Duc Thang University, 19 Nguyen Huu Tho Street, Tan Hung Ward, Ho Chi Minh City, Vietnam

Article info
Type of article:
Original research paper

DOI:
https://doi.org/10.58845/jstt.utt.2026.en.6.2.187-205

***Corresponding author:**
Email address:
htphuoc@ctu.edu.vn

Received: 24/02/2026
Received in Revised Form: 03/04/2026
Accepted: 14/04/2026

Abstract: Developing lightweight and sustainable construction materials is important for reducing the carbon footprint of the construction industry. This study investigated the feasibility of incorporating used coffee grounds (UCG) as a partial replacement for bottom ash (BA), as fine aggregates, in fly ash–ground granulated blast-furnace slag (FA–GGBFS) geopolymer composites. Six mixtures with UCG contents from 0 to 25% by volume were prepared while maintaining constant binder and activator ratios. The effects of UCG on flowability, fresh unit weight, apparent porosity, compressive strength, thermal conductivity, and microstructure were examined. Results showed that 5% UCG improved workability and achieved the highest compressive strength (39.4 MPa, about 15% higher than the control), while maintaining similar thermal conductivity (0.694 W/m·°C). At higher UCG levels (≥15%), porosity increased, and compressive strength decreased markedly, whereas thermal insulation improved, with conductivity decreasing to 0.394 W/m·°C (estimated based on density). SEM observations indicated a compact matrix and dense interfacial transition zone at low UCG contents, while higher replacement levels produced a more porous and discontinuous microstructure. Within the investigated range, 5% UCG yielded the most balanced overall mechanical performance, whereas replacement levels up to 10% provided a practical compromise between weight reduction and thermal insulation, despite a measurable strength penalty relative to the control.

Keywords: Lightweight geopolymer composites (LWGC); used coffee grounds; porosity; compressive strength; thermal conductivity; microstructure.

1. Introduction

The development of sustainable construction materials has become an urgent priority to mitigate global greenhouse gas emissions. The cement industry, fundamental to modern infrastructure, accounts for nearly 8% of total CO_2 emissions worldwide, mainly from clinker production and fossil fuel consumption [1]. In this context,

geopolymer technology, particularly lightweight geopolymer composites (LWGCs), has emerged as a promising alternative to ordinary Portland cement due to its ability to utilize industrial and agricultural by-products rich in aluminosilicate—such as fly ash (FA), ground-granulated blast-furnace slag (GGBFS), and used coffee grounds (UCG)—as effective binders or aggregates, thereby reducing CO_2 emissions by up to 75% during production while enhancing durability and chemical resistance [2]. Beyond sustainability, LWGC is critical for minimizing the structural dead load of high-rise buildings and long-span bridges, which optimizes construction costs and enhances seismic resilience. These materials provide superior thermal and acoustic insulation compared to conventional or normal-weight concrete, leading to improved energy efficiency in building envelopes. Furthermore, LWGC exhibits exceptional durability, maintaining structural integrity under aggressive conditions due to its high resistance to fire, acid attacks, and sulfate exposure [3, 4].

Geopolymers are synthesized through the alkali activation of Si- and Al-rich precursors, forming a stable three-dimensional network of sodium–aluminosilicate–hydrate (N–A–S–H) and/or calcium–aluminosilicate–hydrate (C–A–S–H) gels [5]. Among potential precursors, FA and GGBFS are widely used owing to their high SiO_2, Al_2O_3, and CaO contents, which promote the formation of strong gel structures and early-age strength development [6]. The combination of FA and GGBFS balances the slow reactivity of FA with the high calcium activity of GGBFS, leading to improved mechanical performance and long-term stability [7–12]. However, most studies have focused on dense geopolymer mortars or concretes, whereas LWGC—with advantages in thermal insulation and weight reduction—remains relatively underexplored.

Bottom ash (BA), a by-product of coal-fired power plants, has gained attention as a potential lightweight aggregate due to its porous structure and low bulk density. While BA contributes to reduced unit weight and enhanced thermal insulation, its angular shape and high water absorption can impair workability and compressive strength [13–15]. Moreover, excessive BA content increases porosity and reduces impermeability, leading to lower strength and durability in aggressive environments [6, 13]. Therefore, blending BA with other lightweight waste materials could be a practical strategy to balance density, strength, and durability.

Meanwhile, UCG—an abundant organic waste from the beverage or coffee industry—has attracted interest as an eco-friendly additive for construction materials. UCG possesses low density, a porous structure, and a high carbon content, making it suitable as a lightweight filler or aggregate in alkali-activated systems. Mierzwiński et al. [16] reported that a small UCG addition (≈5%) reduced efflorescence and improved surface stability of fly-ash-based geopolymers, while Şenol [17] observed strength enhancement at low UCG contents but a decline at higher replacements (> 10%) due to increased porosity and matrix discontinuity. Other studies also reported that UCG can improve thermal insulation and reduce density in cementitious or geopolymer materials [18, 19], although its organic nature may inhibit geopolymerization if not properly controlled [20, 21].

Although BA and UCG have been individually incorporated into alkali-activated systems, their combined interaction within FA–GGBFS matrices remains insufficiently understood, particularly regarding the coupled effects on hybrid gel formation, interfacial transition zone integrity, and strength—insulation trade-offs. Existing studies primarily report mechanical or thermal outcomes separately, without systematically linking pore evolution, ITZ behavior, and activator redistribution mechanisms. Addressing this gap is essential because integrating both materials could achieve

an optimal balance between mechanical performance, lightweight characteristics, and thermal efficiency—three essential attributes for sustainable geopolymer composites. Therefore, this study investigates the feasibility of partially replacing BA with UCG in FA–GGBFS-based LWGC. Unlike previous studies that considered BA or UCG individually, this work focuses on their combined interaction within an FA–GGBFS geopolymer system, with particular attention to the coupled effects on pore structure evolution, interfacial transition zone integrity, and the resulting strength–thermal performance trade-off. This integrated approach enables a direct assessment of how combined BA–UCG substitution governs both mechanical performance and thermal behavior through coupled microstructural mechanisms. UCG replacement levels from 0 to 25% by volume were tested to evaluate effects on both engineering performances (i.e., flowability, fresh unit weight (UW), apparent porosity, compressive strength, thermal conductivity), and also microstructural characteristics of LWGC mixtures. The results are expected to provide new insights into the influence mechanisms of UCG in terms of partial BA replacement in FA–GGBFS systems and expand the sustainable utilization of agricultural and industrial by-products in construction materials. Based on this framework and the identified research gap, the following section presents the experimental program, including material selection, mix design, and testing methods used to assess the properties of the LWGC containing both UCG and BA as potential lightweight aggregates.

The valorization of agro-industrial residues such as UCG and BA into structural and semi-structural LWGC represents a viable pathway toward resource circularity and carbon mitigation in the construction sector.

2. Materials and experimental methods

2.1. Materials

The raw materials used in this study included aluminosilicate precursors (binder), an alkaline activator solution, and lightweight aggregates.

First, FA and GGBFS were used as the binder materials in this experiment. Class F FA was collected from the Thermal Power Plant (Southern Vietnam). This material, a by-product of pulverized coal combustion, was captured using electrostatic precipitators and had a specific gravity of 2.27 g/cm^3. In addition, GGBFS supplied by a Steel Company (Central, Vietnam) was obtained by rapid water quenching of molten slag followed by grinding. The GGBFS had a specific gravity of 2.85 g/cm^3. The chemical compositions of FA and GGBFS are presented in Table 1. FA contained high proportions of SiO_2 (50.27%) and Al_2O_3 (35.61%), together with Fe_2O_3 (5.22%), accounting for more than 90% of the total oxides. This composition classifies the FA as Class F according to TCVN 10302:2014 [22] and indicates its suitability as a rich aluminosilicate source for geopolymerization [7, 12]. In contrast, GGBFS exhibited a high CaO content (40.84%) along with SiO_2 (33.87%) and Al_2O_3 (14.41%), suggesting its ability to promote the formation of calcium-based reaction products such as C–A–S–H gel, which can enhance early-age strength [6].

Second, the alkaline activator solution consisted of sodium hydroxide 5M (NaOH) and sodium silicate (Na_2SiO_3), and had densities of 1.19 and 1.38 g/cm^3, respectively.

Finally, the lightweight aggregates were a combination of BA and UCG, in saturated surface dry forms as shown in Fig. 1. BA, collected from the bottom of coal-fired boilers, exhibited a porous structure with a density of 2.15 g/cm³, a fineness modulus of 2.42, and a water absorption of 8.2%. UCG, obtained from coffee industries, was also used as a lightweight fine aggregate. It had a density, fineness modulus, and water absorption of 1.25 g/cm³, 2.24, and 88.7%, respectively.

Fig. 2 presents the scanning electron microscopy (SEM) images of BA and UCG at ×500 magnification (scale bar = 50 μm). The BA particles

exhibited irregular and mostly angular shapes with rough surfaces containing numerous pores and cavities. This porous structure is consistent with the low bulk density and high water absorption of BA. In contrast, the UCG particles showed irregular geometries with a fibrous and cellular morphology, characterized by interconnected voids and small pore channels. Particle agglomeration was also observed, indicating the organic nature and high moisture affinity of this material [18, 19, 21, 23].

Table 1. Chemical compositions of precursor materials

Materials	Primary compositions (wt.%)								
	SiO_2	Al_2O_3	Fe_2O_3	CaO	MgO	SO_3	K_2O	Na_2O	Others
GGBFS	33.87	14.41	0.04	40.84	6.74	1.20	0.47	0.39	4.52
FA	50.27	35.61	5.22	1.20	0.78	0.20	1.87	0.29	2.08

(a) BA (b) UCG

Fig. 1. Lightweight fine aggregates used in this study

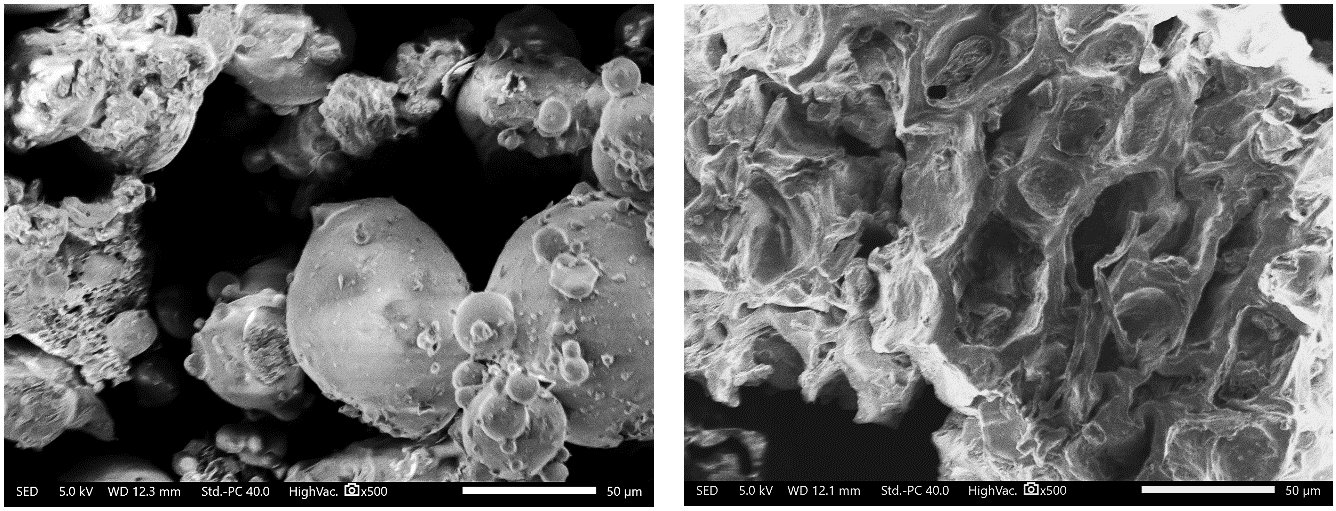

(a) BA (b) UCG

Fig. 2. SEM images of fine aggregates

Furthermore, the local tap water, in compliance with TCVN 4506: 2012 [24], was used for the mixing process.

2.2. Mixture proportions

The LWGCs were designed with constant binder and activator ratios, while varying the replacement level of BA with UCG. Based on the previous research [25, 26], the binder consisted of

FA and GGBFS with a fixed mass ratio of 30/70 in weight %, due to their positive effects on the mechanical properties, and with a relatively dense microstructure of the composites. While the alkaline activator solution (a liquid-to-solid ratio of 0.42) was prepared with NaOH/Na_2SiO_3, corresponding to respective densities of 1.19 and 1.38 g/cm^3. In this experiment, UCG replaced BA as fine aggregates at different levels of 0, 5, 10, 15, 20, and 25% by volume. Moreover, a constant water-to-binder ratio of 0.22 and mixing water dosage of 136 liters/m^3 were used to investigate the influence of UCG contents on the flowability of LWGC mixtures. The detailed proportions of raw materials for all mixtures are summarized in Table 2.

Table 2. Material proportions for the preparation of LWGC

Materials (kg/m^3)	Mixture designation					
	UCG-00	UCG-05	UCG-10	UCG-15	UCG-20	UCG-25
GGBFS	436	436	436	436	436	436
FA	187	187	187	187	187	187
NaOH	94	94	94	94	94	94
Na_2SiO_3	151	151	151	151	151	151
BA	934	888	841	794	747	701
UCG	0	27	54	82	109	136
Water	136	136	136	136	136	136
28-day dry density	1665	1671	1548	1434	1317	1217

2.3. Sample preparation

The mixing procedure was carried out in four steps. First, FA and GGBFS as binders were dry-mixed for 2 min using a laboratory mixer. Subsequently, the activator solution was gradually added, and mixing continued for another 3 min. In the third step, lightweight fine aggregates, such as BA and UCG, were added to the mixer, followed by water, and mixing continued for 3 min to obtain homogeneous mixtures. Before casting, the fresh mixture was tested to examine its flowability and unit weight. Finally, the mixture was placed into 50 × 50 × 50 mm molds. After 24 h, the specimens were demolded and cured under controlled ambient laboratory conditions at 25 ± 2 °C and relative humidity of 60–70% until testing. Fig. 3 illustrates the sample preparation procedure in this research.

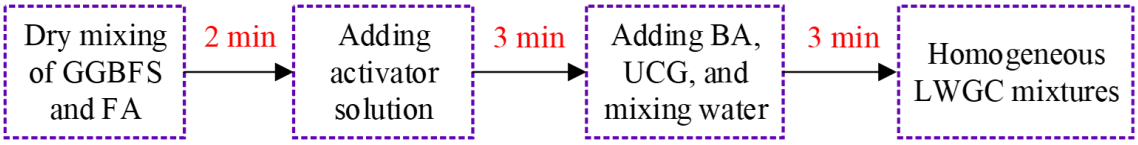

Fig. 3. Mixing process of LWGC mixtures

The mixing procedure for LWGCs generally follows conventional geopolymer mixing protocols; however, strict control is required when incorporating lightweight fine aggregates to prevent segregation due to density differences. The overriding priority is to prevent phase separation, where the lower-density aggregates tend to segregate to the surface [27]. Consequently, obtaining a truly homogeneous mixture relies on the gradual introduction of the lightweight fines into the wet geopolymer paste. This controlled distribution is essential to counter buoyancy effects and ensure the aggregates are uniformly suspended within the hardened composite.

2.4. Testing methods

The fresh properties of the LWGC were evaluated through flowability and fresh UW tests. Flowability was determined using the flow table method (Fig. 4a) in accordance with TCVN 3121-

3:2022 [28]. The spread diameter was measured along two perpendicular directions. The average of these values was reported as the flow. The fresh UW was measured following TCVN 3121-6:2022 [29] by filling a cylindrical container and weighing the container (Fig. 4b). The fresh UW was calculated as the ratio of the net mass of the geopolymer composite to the container volume.

(a) Flowability

(b) Fresh UW

(c) Porosity

(d) Compressive strength

Fig. 4. Properties testing of LWGC

The hardened properties were examined at 28 and 56 days, including apparent porosity, compressive strength, thermal conductivity, and microstructural characteristics. Apparent porosity was determined in accordance with ASTM C642-21 [30] using 50×50×50 mm cubes (Fig. 4c). The specimens were oven-dried at 105°C to constant mass (M_d, g), immersed in water for 48h to obtain the saturated surface-dry mass (M_s, g), and weighed in water (M_{sus}, g). Apparent porosity (P, %) was calculated according to Equation (1):

$$P(\%) = \frac{M_s - M_d}{M_s - M_{sus}} \times 100 \quad (1)$$

Compressive strength was measured in accordance with TCVN 3121-11:2022 [31] using cubes of 50 mm (Fig. 4d). For each mixture, at least

three specimens were tested. The mean compressive strength and corresponding standard deviation were calculated, and all reported results are presented with error bars to reflect experimental variability.

Moreover, thermal conductivity was estimated empirically based on the dry density of LWGC according to ACI 213R-14 [27], as expressed in Equation (2):

$$\lambda = 0.086 \times e^{0.00125D} \ (W/m \cdot {}^oC) \quad (2)$$

where: e = 2.71828, D = dry density of LWGC (kg/m^3)

Table 3. Summary testing properties for evaluating the performance of LWGC

Status of mixture	Criteria	Standards/ References	Notes
Fresh	Flowability	TCVN 3121-3:2022	Once mixing
	Unit weight	TCVN 3121-6:2022	Once mixing
Hardened	Porosity	ASTM C642-21	28 and 56 days
	Compressive strength	TCVN 3121-11:2022	28 and 56 days
	Thermal conductivity	ACI 213R-14	28 days
	Microstructures	Huynh et al. [25]	28 days

It should be noted that the thermal conductivity values were estimated using the empirical relationship proposed by ACI 213R-14 rather than direct measurement. This approach provides a density-based approximation suitable for comparative evaluation among mixtures; however, absolute values may differ from experimentally measured conductivity and should be interpreted accordingly.

Besides, SEM analysis was conducted following similar procedures previously described by Huynh et al. [25]. Microstructural analysis was conducted on fractured surfaces of 28-day-old specimens using a scanning electron microscope at 1000× magnification. Table 3 summarizes the testing to evaluate the engineering performance and microstructures of LWGC in the study.

3. Results and discussion

3.1. Fresh properties

Table 4 presents the fresh properties of geopolymer composites with varying replacement levels of BA by UCG. The flowability ranged from 19 to 22 cm. The reference mixture UCG-00 recorded 19 cm, which increased to 22 cm for UCG-05 and UCG-10 (approximately 15.8% improvement), followed by a slight decrease to 20–21 cm at UCG contents above 10%, corresponding to a reduction of about 4.5–9.1% relative to the peak value. This trend suggests a dual effect of UCG: at low replacement levels, the fine particles and moisture-retention capacity enhanced lubrication and spreadability, whereas at higher contents, the fibrous morphology and large surface area increased inter-particle friction and water absorption, leading to reduced workability [17, 21]. The initial workability enhancement at 5–10% replacement can be attributed to temporary surface lubrication provided by moisture retained within UCG pores. However, as replacement increases, the high absorption capacity (88.7%) progressively reduces free mixing water and increases internal friction, thereby offsetting the lubrication effect and limiting further flow improvement.

The fresh UW consistently decreased with increasing UCG, from 2004 kg/m³ for UCG-00 to 1768 kg/m³ for UCG-25, corresponding to an 11.8% reduction. This decline can be explained by the lower density of UCG (1.25 g/cm³) compared with BA (2.15 g/cm³) and its porous cellular structure, which introduced additional voids into the mixture. Similar reductions in density have been reported for geopolymer systems incorporating lightweight or organic aggregates such as BA and UCG [13, 16, 17]. Lower unit weights can indicate lighter mixes, which might be advantageous for certain situations (i.e., the reduction of the dead load acting on the foundation and structural frame or reduced energy consumption in transportation

and manufacturing).

Overall, UCG contents up to 10% appear to improve flowability without markedly reducing fresh density, while higher levels (≥ 15%) are more effective in lowering density but relatively compromise flowability. These findings indicate that the optimization of UCG content is essential to balance fresh performance with lightweight characteristics in geopolymer composites.

3.2. Apparent porosity

Table 4. Fresh properties of LWGC with varying UCG contents

Mix ID	UCG content (%)	Slump flow (cm)	Fresh UW (kg/m^3)	Fresh UW change (%)
UCG-00	0	19	2004	0.0
UCG-05	5	22	1997	-0.3
UCG-10	10	22	1910	-4.7
UCG-15	15	20	1866	-6.9
UCG-20	20	21	1806	-9.9
UCG-25	25	20	1768	-11.8

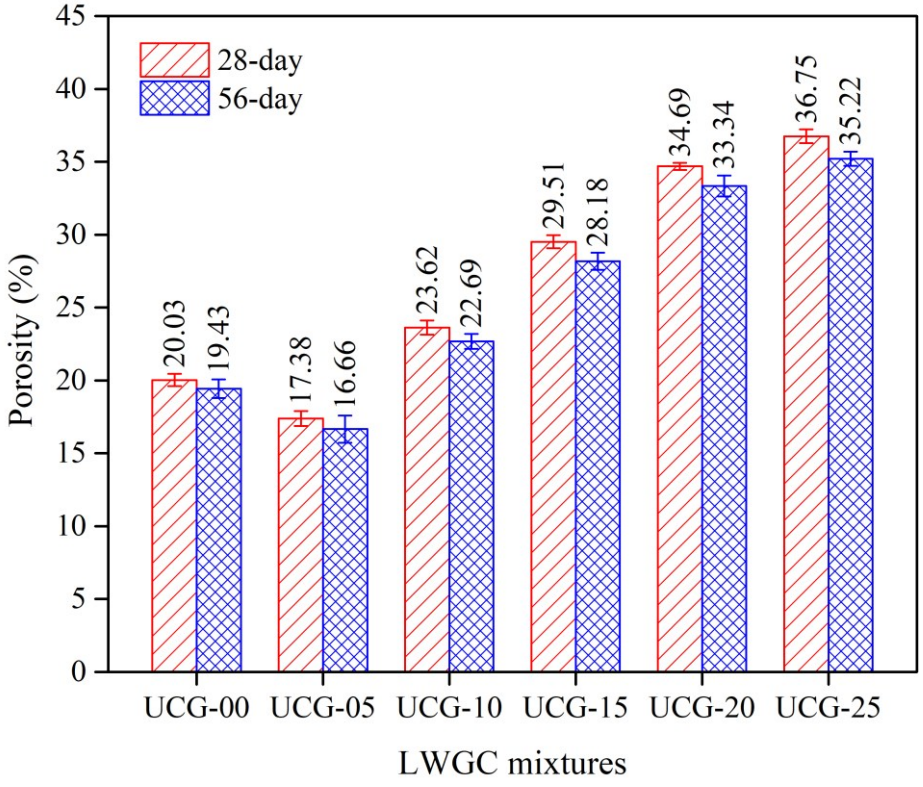

Fig. 5. Porosity of LWGC

Fig. 5 presents the apparent porosity of LWGC incorporating different proportions of UCG as a replacement for BA at 28 and 56 days. In general, an upward trend was observed with increasing UCG content, ranging from 20.03% in UCG-00 to 36.75% in UCG-25 at 28 days. At 56 days, porosity slightly decreased (19.43–35.22%), indicating matrix densification due to continued geopolymerization and gel formation. It can be observed that across curing ages, porosity decreases modestly (3–5% relative) from 28 to 56 days. The reason is that in ambient-cured systems, secondary reactions continue, forming additional C–A–S–H or N–A–S–H gels from CaO in GGBFS that partially fill fine capillary pores. Furthermore, this time-dependent refinement is more pronounced at higher UCG contents, possibly due to delayed activation from organic interferences [19, 21].

At low UCG contents (UCG-05), apparent

porosity decreased from 20.03% (UCG-00, 28 days) to 17.38% (UCG-05, 28 days), and from 19.43% to 16.66% at 56 days, indicating improved particle packing and partial pore refinement at limited replacement levels. In contrast, higher UCG levels (≥ 10%) markedly increased porosity, consistent with previous studies reporting that UCG raises pore volume and water absorption in geopolymer matrices [16, 17]. This behavior is mainly attributed to the fibrous and cellular morphology of UCG. Its organic nature and high moisture affinity also promote microvoid formation during drying [19]. In addition to geometric effects, the organic surface chemistry of UCG may partially delay local geopolymer gel precipitation, resulting in heterogeneous gel distribution and microvoid persistence. Consequently, porosity evolution is governed not only by physical packing but also by local reaction kinetics at the aggregate–matrix interface. These findings are comparable to other lightweight or organic aggregate systems. For example, BA aggregates inherently increase porosity due to their porous structure [13]. Similarly, crumb rubber replacement enhances porosity and water absorption as a result of weak interfacial bonding and internal voids [32]. Such comparisons confirm that UCG behaves similarly to other waste-derived lightweight aggregates, reducing density while promoting higher porosity.

In summary, moderate UCG incorporation (≤ 5%) maintains porosity at acceptable levels while enhancing sustainability and lowering density. Conversely, excessive replacement (≥ 10%) substantially increases porosity, which may negatively affect compressive strength and long-term durability. In fact, the dramatic rise in porosity at 25% replacement (corresponding to an 83.4% increase at 28 days compared with UCG-00) confirms its efficacy for creating LWGC, provided the mechanical requirements of the specific application can tolerate the increased void volume (i.e, non-load-bearing and insulative uses as panels or blocks).

3.3. Compressive strength

Fig. 6 presents the compressive strength development of LWGC containing different proportions of UCGs as a replacement for BA across curing ages. Consistent with the porosity trend discussed in Section 3.2, the compressive strength results show that incorporating a small amount of UCG (≤ 5%) slightly enhanced strength. In contrast, higher replacement levels led to a sharp decline. The control mixture (UCG-00) achieved 34.21 MPa and 35.19 MPa at 28 and 56 days, respectively. With 5% UCG (UCG-05 mixture), the strength increased to 39.42 MPa and 40.14 MPa, approximately 15% higher than the control. However, when the UCG content increased to 10, 15, 20, and 25%, the compressive strength dropped progressively to 28.42–29.52 MPa, 14.29–15.22 MPa, 8.82–9.34 MPa, and 2.23–2.41 MPa at 28 and 56 days, respectively. This trend is consistent with previous studies showing that excessive UCG (> 10%) reduces strength due to higher porosity and discontinuous matrix structure [17, 19].

The continuous strength gain from 28 to 56 days observed in all mixtures indicates ongoing geopolymerization and the secondary formation of N–A–S–H and C–A–S–H gels promoted by GGBFS [6, 20]. In FA–GGBFS systems with high slag content (70 wt.%), the reaction products are typically characterized by a hybrid gel network consisting of C–A–S–H intermixed with N–A–S–H. The coexistence of these phases enhances matrix compactness and load transfer efficiency. Accordingly, the gradual increase in strength from 28 to 56 days is attributed to continued slag hydration and geopolymeric reorganization, rather than to densification alone. Nevertheless, the marked strength reduction with higher UCG content is closely related to the increased apparent porosity (Fig. 5). Conversely, at limited replacement levels (≤ 5%), the rough and irregular surface of UCG particles may provide additional heterogeneous nucleation interfaces for gel

precipitation, primarily through physical surface roughness rather than chemical reactivity. At the same time, this surface texture may enhance mechanical interlocking at low replacement levels. In such cases, the interfacial transition zone (ITZ) may become relatively dense and well bonded, as suggested by the SEM observations in Section 3.5. This improvement in interfacial quality can promote more uniform stress distribution and higher compressive strength than in the control mixture. This interpretation is consistent with the coupled experimental response. At 28 days, porosity decreased from 20.03% in UCG-00 to 17.38% in UCG-05, while compressive strength increased from 34.21 to 39.42 MPa. These results suggest that limited UCG primarily acts through packing refinement and interfacial densification rather than through any intrinsic strengthening of the organic phase. The fibrous, cellular, and highly porous structure of UCG, together with its organic nature and strong water absorption, leads to excessive water uptake during mixing. This high absorption capacity reduces the amount of free liquid available for geopolymerization and alters the effective liquid-to-solid ratio at the local scale, with direct implications for mixture design. Accordingly, pre-treatment or moisture conditioning of UCG prior to mixing may help reduce uncontrolled liquid uptake and improve the stability of the geopolymer matrix, particularly at higher replacement levels. At elevated UCG contents, the resulting reduction in available liquid can limit precursor dissolution and gel formation, thereby contributing to increased porosity and reduced mechanical performance.

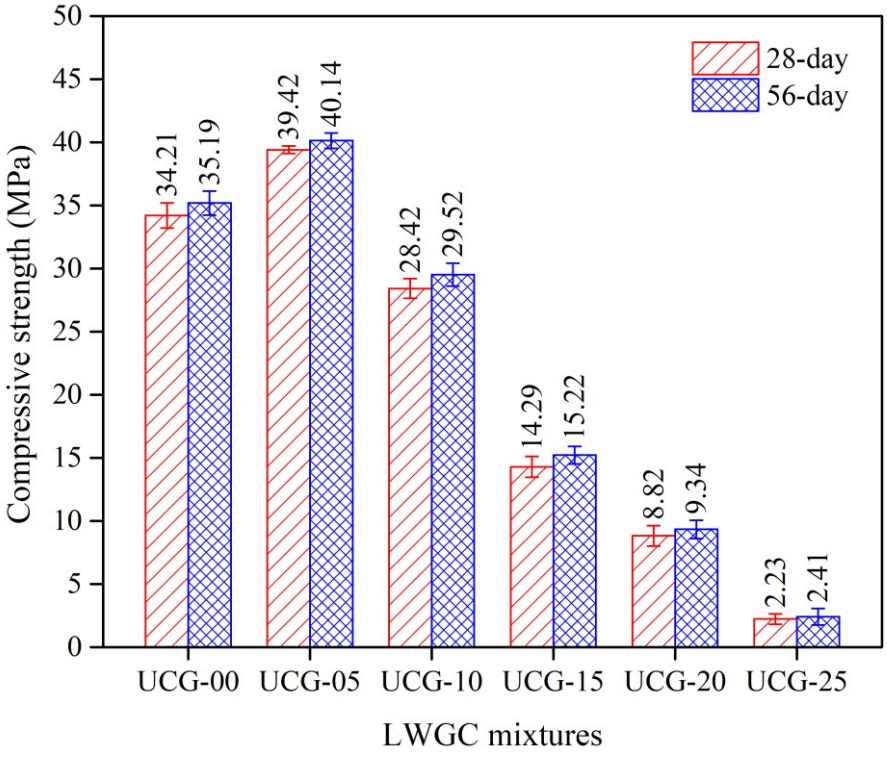

Fig. 6. Compressive strength of LWGC

From a micromechanical standpoint, the ITZ between UCG particles and the surrounding geopolymer matrix governs the load transfer efficiency under compressive stress. Unlike inert mineral aggregates, UCG exhibits a highly porous and organic surface texture that can absorb part of the alkaline solution, thereby locally reducing the effective activator concentration at the particle–matrix interface. This localized depletion may hinder the formation of a continuous C–A–S–H/N–A–S–H gel network in the vicinity of UCG particles. As a result, a relatively weak and porous ITZ develops, which acts as a preferential site for crack initiation and propagation under load. Upon curing,

the absorbed water evaporates, forming micro-voids and fine cracks that weaken the interfacial transition zone between UCG particles and the geopolymer matrix [23]. The presence of these interfacial defects promotes stress concentration under compressive loading. Once microcracks initiate within the ITZ, they can rapidly coalesce due to the relatively low stiffness and cohesive strength of the organic inclusion. Consequently, failure becomes governed by interfacial debonding rather than matrix crushing, explaining the pronounced strength reduction observed at UCG contents ≥ 15%. This behavior is consistent with fracture mechanics principles in LWGC containing porous inclusions, where the ITZ often represents the weakest link in the composite system. Moreover, the presence of organic constituents may interfere with local gel precipitation kinetics through adsorption and physical retention effects rather than direct chemical participation. In addition, the exceptionally high water absorption of UCG (88.7%) implies that part of the activator-bearing pore solution may be physically retained within the organic pores during mixing. This reduces the free liquid available for precursor dissolution. This activator starvation effect can lower the local pH and silicate availability at the particle–matrix vicinity, thereby suppressing gel precipitation and amplifying ITZ porosity. The resulting microstructural heterogeneity provides a mechanistic explanation for why strength drops sharply beyond 10–15% replacement even though the overall binder and nominal activator ratios remain constant. Therefore, the deterioration of mechanical performance at high UCG contents cannot be interpreted solely as a density effect. Instead, it reflects a multiscale degradation mechanism involving reduced effective alkalinity, incomplete gel connectivity, and weakened interfacial bonding.

In literature, comparable phenomena have been reported in geopolymers containing other lightweight or organic aggregates such as BA or crumb rubber, where increased porosity reduces compressive strength but contributes to lower density and improved thermal insulation [13, 32]. Compared with these systems, UCG exhibits a more pronounced effect owing to its higher organic content and finer, more porous texture, leading to a steeper strength decline at high replacement levels. Overall, the mechanical performance of LWGCs containing UCG is therefore governed by a coupled mechanism involving matrix densification, pore structure evolution, and ITZ integrity. While bulk porosity controls the global stiffness and load-bearing capacity, the microstructural quality of the particle–matrix interface determines crack initiation resistance. The strong linear correlation between apparent porosity and compressive strength (R^2 = 0.985) thus reflects not only volumetric void content but also the progressive degradation of interfacial bonding as UCG content increases.

From an application standpoint, the experimental results suggest distinct performance domains across the investigated replacement range. UCG-05, with a 28-day compressive strength of nearly 40 MPa and a dry density of 1671 kg/m³, falls within the range commonly reported for structural-grade lightweight cementitious materials [27]. UCG-10 to UCG-15, with strengths of approximately 15–28 MPa and 28-day dry densities of 1317–1548 kg/m³, may be more suitable for masonry units, pavers, or internal partition walls. In contrast, UCG-20 to UCG-25, with strengths below 10 MPa, are not suitable for load-bearing use. Nevertheless, their high porosity and low dry density (1217–1317 kg/m³) indicate potential for thermal insulation panels or lightweight acoustic barriers, where strength is secondary to weight reduction.

Moreover, a quantitative relationship between apparent porosity and compressive strength is illustrated in Fig. 7. The linear regression model ($y = 72.609 – 1.928x$, $R^2 = 0.985$) demonstrates an excellent inverse correlation,

indicating that each 1 % increase in porosity results in an approximate 1.93 MPa loss in compressive strength. This strong relationship confirms that matrix densification is the dominant factor controlling mechanical performance. However, it should be emphasized that bulk porosity quantified by ASTM C642-21 represents open and connected voids at the macro-scale, whereas mechanical degradation at higher UCG contents is also strongly governed by localized interfacial porosity within the ITZ. Therefore, the linear correlation reflects not only volumetric void content but also progressive deterioration of interfacial continuity, which cannot be directly quantified by global porosity measurement alone. Therefore, limiting the UCG replacement level to ≤ 10% is recommended to maintain adequate strength while achieving a desirable lightweight structure and improved sustainability through waste utilization.

3.4. Thermal conductivity

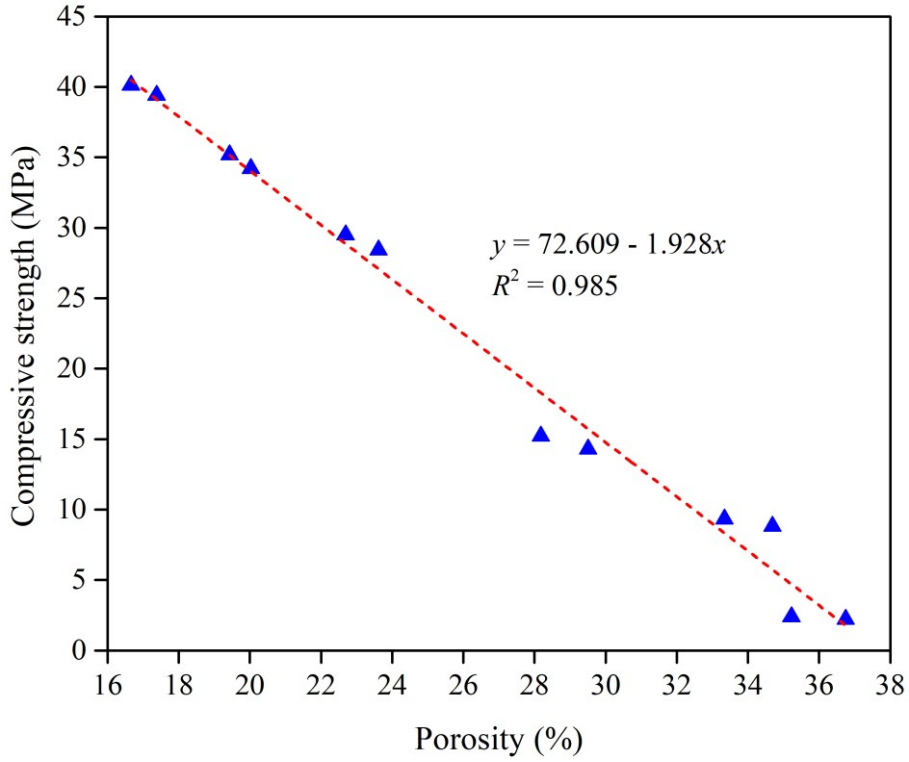

Fig. 7. Correlation between porosity and compressive strength of LWGC

Fig. 8 demonstrates the thermal conductivity of LWGCs incorporating various UCG contents as a BA replacement. The results show a clear decreasing trend with increasing UCG content, aligned with the trend of porosity development in Section 3.2. In this experiment, thermal conductivity decreased from 0.689 W/m·°C for the control mixture (UCG-00) to 0.394 W/m·°C for UCG-25, representing an overall reduction of approximately 43%. A slight fluctuation was observed at 5% UCG (0.694 W/m·°C, less than 1% difference), but the decline became more pronounced beyond 10%. This behavior agrees with previous studies showing that thermal conductivity decreases as bulk density decreases [18, 21, 32]. This trend can be attributed to microstructural modifications induced by UCG addition. The lower dry density (Table 2) and higher apparent porosity (Fig. 5) result from the porous and fibrous morphology of UCG, which introduces numerous air voids into the geopolymer matrix. Such voids act as effective thermal barriers, impeding heat transfer through the solid phase [16]. Similar effects have been observed in other organic or agricultural-based lightweight aggregates, where the cellular texture increases pore volume and decreases heat flow [23]. At moderate replacement levels (≤ 10%), the

composites maintained sufficient matrix integrity while exhibiting noticeably improved insulation performance. However, when the UCG content exceeded 15%, the higher porosity and weaker interfacial bonding further reduced thermal conductivity but simultaneously weakened compressive strength. A comparable relationship between density, porosity, and insulation efficiency was reported in crumb-rubber-based geopolymers [32].

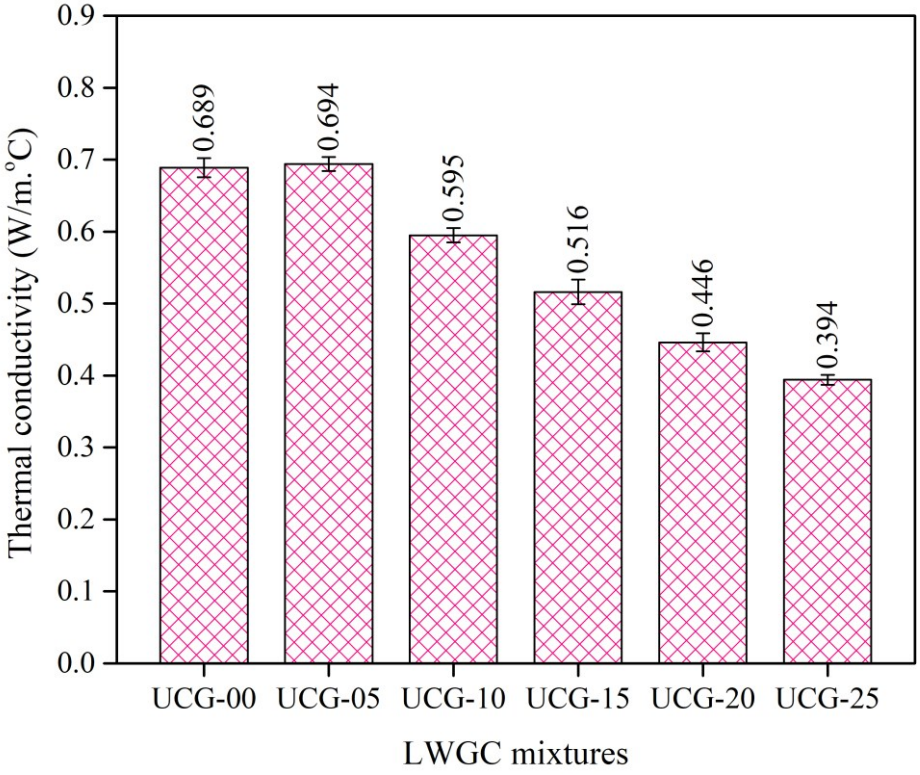

Fig. 8. Thermal conductivity of LWGC

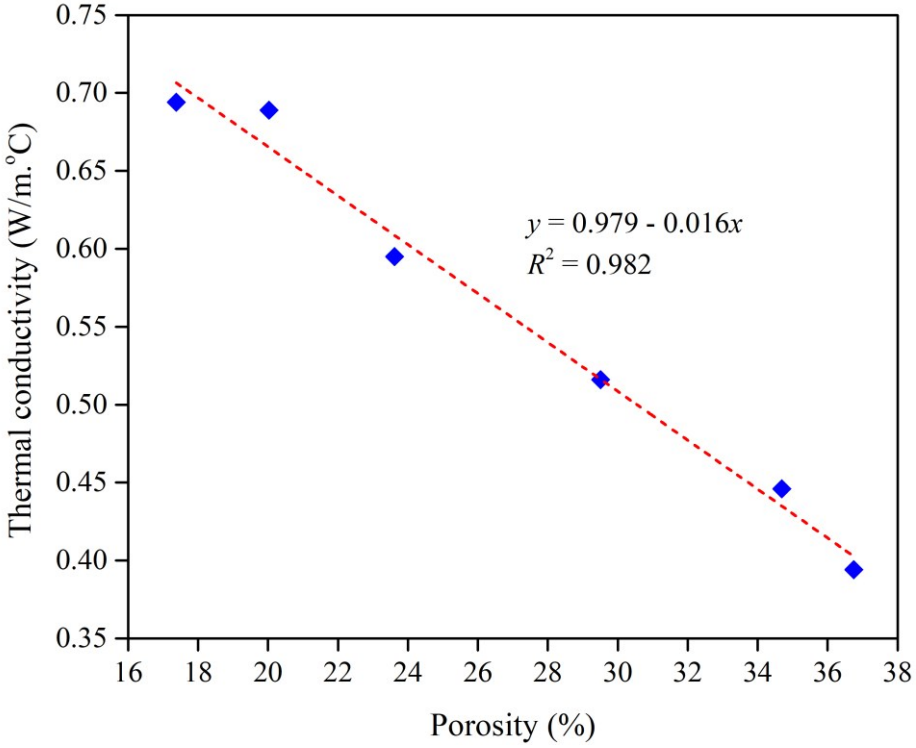

Fig. 9. Correlation between porosity and thermal conductivity of LWGC

The estimated thermal conductivity values, calculated based on the empirical density relationship (Equation 2), showed internal consistency with the observed density–porosity trends. Fig. 9 presents the correlation between thermal conductivity and apparent porosity, expressed by the regression equation $y = 0.979 - 0.016x$ ($R^2 = 0.982$). Each 1% increase in porosity corresponds to an approximate 0.016 W/m·°C reduction in thermal conductivity, indicating that porosity is the dominant factor governing thermal behavior [13, 19].

3.5. SEM observations

Fig. 10 presents SEM micrographs (×1000, scale bar = 10 μm) of LWGC in which BA was progressively replaced by UCG from 0 to 25%. The image sequence (a–f) illustrates the microstructural evolution of the geopolymer matrix with increasing UCG content and its relationship with gel continuity, matrix compactness, and the resulting mechanical and thermal behavior. For instance, in the UCG-00 sample (Fig. 10a), the matrix exhibited a dense, homogeneous, and well-bonded morphology with only a few isolated micropores. Spherical FA particles were fully embedded within a continuous aluminosilicate and calcium–aluminosilicate gel framework, reflecting effective geopolymerization. This compact morphology corresponded to a porosity of 20.03%, compressive strength of 34.21 MPa, and thermal conductivity of 0.689 W/m·°C, consistent with the findings of Topçu et al. [33], who emphasized the role of a continuous gel phase in enhancing mechanical and chemical stability.

At 5% UCG replacement (Fig. 10b), the matrix remained compact but became more uniform due to the fine distribution of UCG particles. Small voids were partially filled with gel, forming a dense and coherent interfacial transition zone (ITZ). This refined texture resulted in the lowest porosity (17.38% at 28 days), highest compressive strength (39.42 MPa at 28 days), and stable thermal conductivity (0.694 W/m·°C at 28 days). Similar observations were reported by Şenol [17] and Mierzwiński et al. [16], who found that a small UCG addition can refine the pore structure, enhance matrix homogeneity, and improve particle–gel bonding. As UCG content increased to 10% (Fig. 10c), the gel became less uniform, and several small pore clusters began to coalesce. The coating around UCG particles was partly discontinuous, leading to localized detachment and the formation of fine cracks. Consequently, porosity increased to 23.62%, compressive strength decreased to 28.42 MPa, and thermal conductivity dropped to 0.595 W/m·°C. This behavior reflects weakened ITZ bonding due to water absorption by UCG, similar to the mechanism described by Khong et al. [19], who observed that excessive organic content can absorb water and alkali, hinder gel formation, and generate voids during drying. On the other hand, the UCG-25 sample (Fig. 10f) displayed a severely porous network, with minimal gel coverage and weak particle contacts. The structure was dominated by interconnected cavities, yielding the highest porosity (36.75%), lowest strength (2.23 MPa), and lowest conductivity (0.394 W/m·°C). The open-cell texture is comparable to that reported by Wongsa et al. [13], where highly porous geopolymer mortars exhibited excellent insulation but limited load-bearing capacity.

The progressive transformation observed across the six micrographs suggests that BA substitution with UCG modifies the continuity of the geopolymer gel network. At low replacement levels (≤ 10%), UCG primarily acts as a fine filler, and its rough surface may provide heterogeneous nucleation interfaces for gel precipitation through physical surface roughness rather than intrinsic chemical reactivity, thereby contributing to improved ITZ bonding. At higher levels (> 15%), its porous organic nature increases water absorption and evaporation during curing, generating microvoids and reducing gel integrity (Figs. 10d and 10e). This mechanism is consistent with the

work of Arulrajah et al. [23], who reported that UCG and other organic residues can disrupt gel continuity when present in excess.

The SEM observations align closely with the quantitative results: porosity rose from 20.03% to 36.75%, while compressive strength declined from 34.21 MPa to 2.23 MPa, and thermal conductivity decreased from 0.689 to 0.394 W/m·°C. It should be noted that the SEM analysis provides qualitative microstructural evidence based on localized regions, and quantitative pore size distribution or ITZ thickness measurements would require complementary techniques such as MIP or image analysis for full validation. These complementary methods would be valuable in future work to quantify pore connectivity, pore size distribution, and interfacial characteristics more rigorously. The nearly linear correlations ($R^2 \approx 0.98$) indicate that matrix compactness governs both mechanical and thermal performance. A denser gel network transmits stress and heat more effectively, whereas a highly porous matrix reduces thermal conductivity but weakens the material's load-bearing capacity. This strength–insulation trade-off typifies lightweight geopolymers with organic or cellular inclusions [4, 32]. This inherent trade-off underscores the importance of defining application-specific optimization criteria rather than pursuing strength or insulation performance independently.

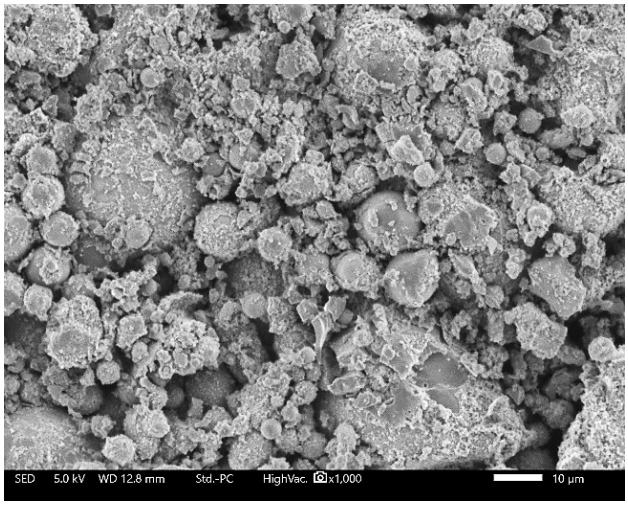

(a) UCG-00

(b) UCG-05

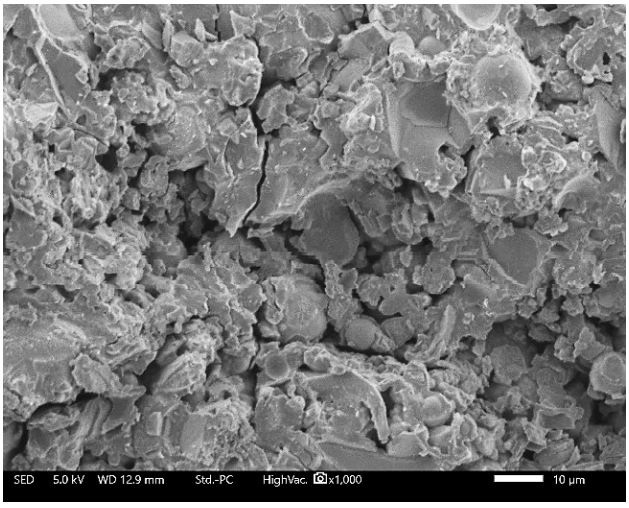

(c) UCG-10

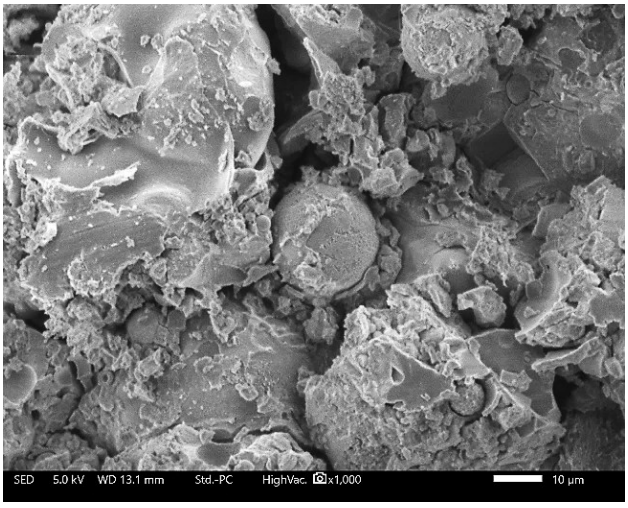

(d) UCG-15

Fig. 10. SEM morphologies of LWGC (×1000, scale bar = 10 µm) with different UCG replacement levels ranging from 0 to 25% by volume at the age of 28 days

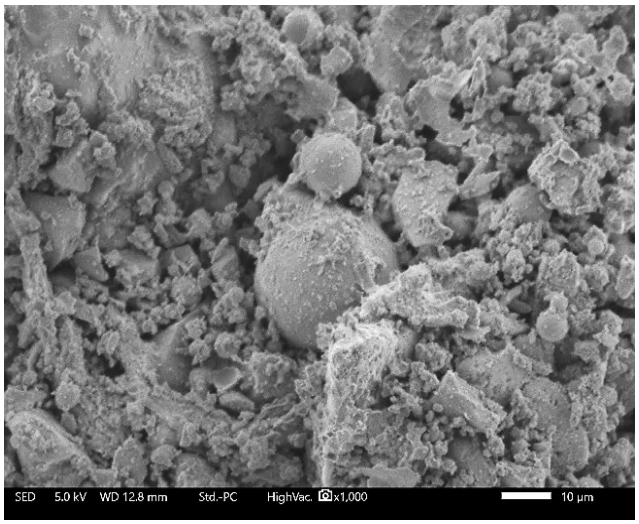

(e) UCG-20

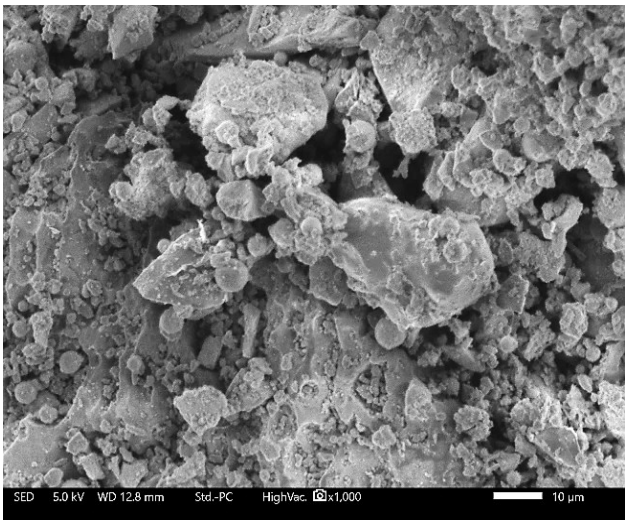

(f) UCG-25

Fig. 10. (continued)

Overall, the SEM analysis confirms that a UCG content of up to 10% maintains a continuous gel framework and strong ITZ bonding, achieving low porosity, high strength, and stable thermal behavior. Beyond this threshold, the matrix becomes increasingly open and porous, leading to a significant loss in mechanical integrity but improved insulation. These findings support the interpretation that UCG acts as both a lightweight filler and an organic modifier, highlighting the balance between mechanical performance, thermal efficiency, and sustainability in FA–GGBFS geopolymer composites, consistent with the trends reported by Şenol [17], Mierzwiński et al. [16], and Khong et al. [19].

4. Conclusions

This study investigated the feasibility of utilizing UCG as a partial replacement for BA in FA–GGBFS-based LWGC. The experimental program evaluated the effects of UCG content (0–25% by volume) on flowability, fresh UW, apparent porosity, compressive strength, thermal conductivity, and microstructure characteristics, aiming to develop lightweight and sustainable geopolymer materials. Based on the experimental findings, the following conclusions can be drawn:

- Incorporation of UCG at 5% by volume improved flowability (19 to 22 cm) and increased 28-day compressive strength from 34.21 MPa (UCG-00) to 39.42 MPa (≈15% higher). At 10% replacement, flowability remained high (22 cm), but compressive strength decreased to 28.42 MPa, indicating that workability enhancement does not necessarily translate to strength retention at higher UCG dosages.

- Apparent porosity increased with higher UCG contents due to the fibrous and cellular morphology of UCG, while small additions (≤ 5% in the case of UCG-05 mixture) refined the matrix and maintained compactness similar to the control (UCG-00), corresponding to a 13.2% relative reduction at 28 days compared with UCG-00.

- Compressive strength reached an optimum at 5% UCG (≈39.4 MPa, ≈15% higher than the control UCG-00), whereas further addition led to a significant reduction (up to 93%) due to increased porosity (up to ≥ 80%) and weak interfacial bonding.

- Thermal conductivity of LWGC decreased from 0.689 W/m·°C (UCG-00) to 0.394 W/m·°C (UCG-25), confirming the role of UCG in improving thermal insulation. Besides, SEM observations revealed a dense, well-bonded matrix at low UCG levels (≤ 5%), and a porous, discontinuous network at high contents (> 10%).

- Within the investigated range, UCG-05 exhibited the most balanced overall performance. This mixture showed improved workability, the

highest compressive strength (39.4 MPa), and thermal conductivity comparable to that of the control (0.694 W/m·°C).

- The mechanical–thermal performance transition is governed by a coupled mechanism involving hybrid gel evolution, pore connectivity development, and ITZ integrity. Limited UCG enhances packing and interfacial densification, whereas excessive replacement induces activator redistribution and interfacial debonding, leading to porosity-driven strength degradation.

Overall, within the scope of the present study, UCG replacement up to 10% by volume appears to provide a reasonable upper range for maintaining acceptable mechanical performance while achieving meaningful density reduction and improved thermal insulation. Beyond this level, performance becomes increasingly governed by porosity-driven microstructural discontinuity and ITZ degradation. This study is limited to ambient curing conditions and density-based estimation of thermal conductivity. Direct thermal measurements and long-term durability assessments (i.e., water absorption kinetics, shrinkage, and freeze–thaw resistance) are recommended to comprehensively evaluate practical applicability.

Acknowledgment

The authors would like to thank the Huynh's research group at Can Tho University for their assistance during the experimental work.

References

[1] S. Philip, M. Nidhi. (2023). A review on the material performance of geopolymer concrete as green building materials. *Materials Today: Proceedings*. (In Press). https://doi.org/10.1016/j.matpr.2023.04.110

[2] R.R. Bellum, C.S.S. Durga, K. Meeravali, N.S.V. Kumar, B.K. Chaitanya, C. Venkatesh. (2025). A comprehensive review of geopolymer concrete: applications, properties, and future directions. *Silicon*, 18, 807–843. https://doi.org/10.1007/s12633-025-03532-z

[3] M.A. Khasawneh. (2025). Geopolymer concrete in construction projects: a review. *Discover Civil Engineering*, 2, 124. https://doi.org/10.1007/s44290-025-00281-1

[4] M.S.T. Masoule, N. Bahrami, M. Karimzadeh, B. Mohasanati, P. Shoaei, F. Ameri, T. Ozbakkaloglu. (2022). Lightweight geopolymer concrete: A critical review on the feasibility, mixture design, durability properties, and microstructure. *Ceramics International*, 48(8), 10347–10371. https://doi.org/10.1016/j.ceramint.2022.01.298

[5] L.M. Deraman, M.M. Al Bakri Abdullah, Y. Liew, K. Hussin, Z. Yahya. (2015). A review on processing and properties of bottom ash based geopolymer materials. *Key Engineering Materials*, 660, 3–8. https://doi.org/10.4028/www.scientific.net/KEM.660.3

[6] N. Bheel, M. Alwetaishi, I.A. Jae, A. Syamsir, et al. (2024). Enhancing performance and sustainability of GGBFS-based self-compacting geopolymer concrete blended with coal bottom ash and metakaolin by using RSM modelling. *Scientific Reports*, 14, 19754. https://doi.org/10.1038/s41598-024-70800-0

[7] G. Mallikarjuna Rao, T.D. Gunneswara Rao. (2018). A quantitative method of approach in designing the mix proportions of fly ash and GGBS-based geopolymer concrete. *Australian Journal of Civil Engineering*, 16(1), 53–63. https://doi.org/10.1080/14488353.2018.1450716

[8] Y. Saeki, K. Fujikake, T. Sasatani, N. Kuwahara, D. Kuroiwa, (2022). Development of cast-in-place FA-GGBFS-based geopolymer mortar: an experimental study. *Practice Periodical on Structural Design and Construction*, 27(2), 04022009.https://doi.org/10.1061/(ASCE)SC.1943-5576.0000681

[9] R.R. Bellum, K. Muniraj, S.R.C. Madduru. (2020). Exploration of mechanical and durability characteristics of fly ash-GGBFS based green geopolymer concrete. *SN Applied*

Sciences, 2, 919. https://doi.org/10.1007/s42452-020-2720-5

[10] H. El-Hassan, N. Ismail. (2018). Effect of process parameters on the performance of fly ash/GGBS blended geopolymer composites. J. Sustain. *Journal of Sustainable Cement-Based Materials*, 7(2), 122–140. https://doi.org/10.1080/21650373.2017.1411296

[11] J. Xie, J. Wang, R. Rao, C. Wang, C. Fang. (2019). Effects of combined usage of GGBS and fly ash on workability and mechanical properties of alkali activated geopolymer concrete with recycled aggregate. *Composites Part B: Engineering*, 164, 179–190. https://doi.org/10.1016/j.compositesb.2018.11.067

[12] P. Zhang, Z. Gao, J. Wang, J. Guo, S. Hu, Y. Ling. (2020). Properties of fresh and hardened fly ash/slag based geopolymer concrete: A review. *Journal of Cleaner Production*, 270, 122389. https://doi.org/10.1016/j.jclepro.2020.122389

[13] A. Wongsa, Y. Zaetang, V. Sata, P. Chindaprasirt. (2016). Properties of lightweight fly ash geopolymer concrete containing bottom ash as aggregates. *Construction and Building Materials*, 111, 637–643. https://doi.org/10.1016/j.conbuildmat.2016.02.135

[14] N. Ankur, N. Singh. (2021). Performance of cement mortars and concretes containing coal bottom ash: A comprehensive review. *Renewable and Sustainable Energy Reviews*, 149, 111361. https://doi.org/10.1016/j.rser.2021.111361

[15] T.P. Huynh, S.H. Ngo, V.-D. Nguyen. (2024). Utilizing coal combustion bottom ash as a sustainable alternative to natural aggregate in eco-friendly building bricks. *CTU Journal of Innovation and Sustainable Development*, 16 (Special issue: ICCEE), 1–7. https://doi.org/10.22144/ctujoisd.2024.274

[16] D. Mierzwiński, K. Korniejenko, M. Łach, J. Mikuła, J. Krzywda. (2018). Effect of coffee grounds addition on efflorescence in fly ash-based geopolymer. *IOP Conference Series: Materials Science and Engineering*, 416, 012035. https://doi.org/10.1088/1757-899X/416/1/012035

[17] A.F. Şenol. (2025). Performance of geopolymer mortar incorporating spent coffee grounds as a recycled building material: An experimental and predictive analysis. *Hybrid Advances*, 10, 100479. https://doi.org/10.1016/j.hybadv.2025.100479

[18] A. Lachheb, A. Allouhi, M. El Marhoune, R. Saadani, et al. (2019). Thermal insulation improvement in construction materials by adding spent coffee grounds: An experimental and simulation study. *Journal of Cleaner Production*, 209, 1411–1419. https://doi.org/10.1016/j.jclepro.2018.11.140

[19] S.C. Khong, J.J. Yee, J. Gimbun, K.F. Tee, S.C. Chin. (2025). Spent coffee grounds enhanced strength of alkali-hydroxide-free geopolymer concrete: an optimization study. *Journal of Materials Science: Materials in Engineering*, 20, 109. https://doi.org/10.1186/s40712-025-00331-7

[20] T.-A. Kua, A. Arulrajah, S. Horpibulsuk, Y.-J. Du, S.-L. Shen. (2016). Strength assessment of spent coffee grounds-geopolymer cement utilizing slag and fly ash precursors. *Construction and Building Materials*, 115, 565–575.https://doi.org/10.1016/j.conbuildmat.2016.04.021

[21] M. Saeli. (2025). Chapter 12 - Performance of cementitious composites based on spent coffee ground. *Advances in Bio-Based Materials for Construction and Energy Efficiency, Woodhead Publishing Series in Civil and Structural Engineering*, 2025, pp. 297–336. https://doi.org/10.1016/B978-0-443-32800-8.00010-X

[22] Ministry of Science and Technology,

Vietnam. (2014). TCVN 10302:2014. Activity admixture – Fly ash for concrete, mortar and cement (in Vietnamese).

[23] A. Arulrajah, T.-A. Kua, C. Suksiripattanapong, S. Horpibulsuk, J.S. Shen. (2017). Compressive strength and microstructural properties of spent coffee grounds-bagasse ash based geopolymers with slag supplements. *Journal of Cleaner Production*, 162, 1491–1501. https://doi.org/10.1016/j.jclepro.2017.06.171

[24] Ministry of Science and Technology, Vietnam. (2012). TCVN 4506:2012. Water for concrete and mortar – Technical specification (in Vietnamese).

[25] T.H.Y. Nguyen, N.T. Cao, T.D.M. Ngoc, T.-P. Huynh. (2022). Experimental evaluation on engineering properties and drying shrinkage of no-cement mortar produced by alkaline activation of fly ash-slag mixtures. *Engineering Journal*, 26(3), 17–28. https://doi.org/10.4186/ej.2022.26.3.17

[26] Q.D. Huynh, H.N.H. Luong, N.T. Ngo, T.H. Duong, et al. (2025). Recycling used coffee grounds as fine aggregate in alkali-activated lightweight non-load-bearing composites. *CTU Journal of Innovation and Sustainable Development*, 17(Special issue: ETMD), 24–31. https://doi.org/10.22144/ctujoisd.2025.004

[27] American Concrete Institute. (2014). ACI 213R-14, Guide for structural lightweight-aggregate concrete.

[28] Ministry of Science and Technology, Vietnam. (2022). TCVN 3121-3:2022. Mortar for masonry – Test methods – Part 3: Determination of consistence of fresh mortar (by flow table). (in Vietnamese).

[29] Ministry of Science and Technology, Vietnam. (2022). TCVN 3121-6:2022. Mortar for masonry – Test methods – Part 6: Determination of bulk density of fresh mortar. (in Vietnamese).

[30] ASTM International. (2021). ASTM C642-21. Standard test method for density, absorption, and voids in hardened concrete.

[31] Ministry of Science and Technology, Vietnam. (2022). TCVN 3121-11:2022. Mortar for masonry – Test methods – Part 11: Determination of flexural and compressive strength of hardened mortars. (in Vietnamese).

[32] A. Wongsa, V. Sata, B. Nematollahi, J. Sanjayan, P. Chindaprasirt. (2018). Mechanical and thermal properties of lightweight geopolymer mortar incorporating crumb rubber. *Journal of Cleaner Production*, 195, 1069–1080. https://doi.org/10.1016/j.jclepro.2018.06.003

[33] İ.B. Topçu, M.U. Toprak, T. Uygunoğlu. (2014). Durability and microstructure characteristics of alkali activated coal bottom ash geopolymer cement. *Journal of Cleaner Production*, 81, 211–217. https://doi.org/10.1016/j.jclepro.2014.06.037